# Comparison of Infrared Atmospheric Brightness Temperatures Measured by a Fourier Transform Spectrometer and a Filter Radiometer

JOSEPH A. SHAW, JACK B. SNIDER, JAMES H. CHURNSIDE, AND MARK D. JACOBSON

*Environmental Technology Laboratory, National Oceanic and Atmospheric Administration, U.S. Department of Commerce, Boulder, Colorado*

12 October 1994 and 27 March 1995

ABSTRACT

Increased interest in using atmospheric brightness temperature measurements from simple infrared radiometers combined with radars and lidars has prompted the investigation of their accuracy for various sky conditions. In comparisons of atmospheric brightness temperatures (Tb) measured by a Fourier transform infrared (FTIR) spectrometer and a single-band filter radiometer (PRT5), the authors establish that the PRT5 measurements agree with those from the more sophisticated and accurate FTIR within 1.5 K rms over the range where both instruments are calibrated. Below the PRT5's cold calibration cutoff of 205 K, the PRT5 measures too warm. The FTIR, which is calibrated over the entire measurement range, provides a calibration for the erroneous PRT5 measurements, enabling quantitative use of the simple and inexpensive PRT5 over a larger, more useful range. The corrected data agree within 1.5 K rms, with over 90% differing by less than one temporal standard deviation. The calibration correction technique is applicable to a variety of radiometers and most importantly shows that PRT5-type radiometers are indeed capable of accurately measuring clear-sky and cirrus emission.

## 1. Introduction

Infrared emission measurements are becoming critical components of atmospheric research, particularly when combined with complementary measurements. Matrosov et al. (1994) and Uttal et al. (1994) combined data from a PRT5 infrared radiometer and a microwave radar to infer microphysical and radiative properties of cirrus clouds. Ackerman et al. (1990), Spinhirne and Hart (1990), Grund et al. (1990), Platt (1973), and Platt and Dilley (1981) combined infrared radiometers and lidars to infer cloud optical properties.

To assess the PRT5's capabilities, Snider (1987) compared brightness temperatures from PRT5 infrared radiometers (1-min averages) with radiosonde temperatures at stratus cloud heights, demonstrating rms differences of 1.2 K with a 1.1 K bias. Shaw and Fedor (1993) improved the calibration technique and showed rms uncertainties less than 1 K in 30-s measurements of stratus clouds. However, until now there has been no independent verification that a PRT5-style radiometer can accurately measure emissions from cirrus clouds or the clear atmosphere.

During the First ISCCP (International Satellite Cloud Climatology Project) Radiation Experiment II (FIRE II) experiment in Coffeyville, Kansas, in November and December 1991, we operated two infrared radiometric systems that are of fundamentally different design and calibrated them using independent techniques. The first instrument is a modified Barnes PRT5 radiometer (PRT5) and the second is a Fourier transform infrared (FTIR) spectrometer configured as an emission spectroradiometer. The FTIR measured spectral radiance at high spectral resolution (1 $cm^{-1}$) and low temporal resolution (3–4 min), while the PRT5 measured equivalent brightness temperature over a 1.48-$\mu$m band, centered at 10.7 $\mu$m, with high temporal resolution (30 s, occasionally 5 s).

In this paper, we compare equivalent brightness temperatures Tb measured by these two instruments from 13 November 1991 to 28 November 1991. To facilitate this comparison, we integrated the FTIR measurements to match the spectral bandwidth of the PRT5 and averaged the PRT5 measurements to match the integration period of the FTIR. These data agree within 1.5 K rms for Tb > 205 K, but for colder temperatures the PRT5 measurements are too warm. The poor comparison at low temperatures was expected because the PRT5 is calibrated only down to about 205 K. We use the well-calibrated FTIR measurements to provide an extended cold calibration for the PRT5, verifiable with radiative transfer calculations. The resulting data exhibit an rms difference of 1.5 K over the entire range with no bias.

*Corresponding author address:* Joseph Shaw, NOAA/ETL, R/E/ET5, 325 Broadway, Boulder, CO 80303-3328.
E-mail: jshaw@etl.noaa.gov

## 2. Description of the instruments

### a. *Fourier transform infrared spectrometer (FTIR)*

A Fourier transform spectrometer infers an autocorrelation of the incident radiation by measuring the strength of the central interference fringe as a function of the optical path difference in a Michelson interferometer. The Fourier transform of this interferogram produces the power spectrum of the incident light. During FIRE II, our FTIR measured zenith emission between 500 and 2000 $cm^{-1}$ (20–5-$\mu$m wavelength) with 1-$cm^{-1}$ spectral resolution and a full-angle field of view of 35 mrad.

The raw atmospheric emission spectrum is calibrated using measurements of two blackbody sources, after the manner of Revercomb et al. (1988). The calibration sources are high-emissivity cavities operating at temperatures that bracket the range of expected atmospheric brightness temperatures: one near ambient temperature ($\approx$300 K) and the other at 77 K. A calibrated atmospheric spectrum is collected once every 12 min, of which time 3 min and 40 s are spent viewing the atmosphere.

A characteristic of the FTIR optics that could be important in this comparison is that the entrance pupil, rather than the emission source, is imaged at the detector to minimize the effects of spatial inhomogeneities in the HgCdTe detector's response. With this design, a cloud that fills part of the instrument's field of view illuminates the entire detector; without it, the signal would fluctuate as the cloud image moved across the detector surface.

During FIRE II, we operated the FTIR almost continuously. Between 13 and 28 November 1991, we collected 403 atmospheric spectra, all of which are included in this discussion.

### b. *Single-band filter radiometer (PRT5)*

In an adjacent trailer, within 10 m from the FTIR, we operated a Barnes PRT5 radiometer that has been modified to have a narrower spectral bandpass with 3-dB cutoff wavelengths of 9.948 and 11.428 $\mu$m, and to have maximum gain at the low-temperature end without saturating the ambient temperature response. This simple, compact radiometer uses a bolometer detector with no cryogens. The full field-of-view angle is approximately the same as the FTIR (35 mrad). A rotating reflective chopper maintains a gain calibration as long as the detector temperature is constant.

We calibrate our PRT5 radiometers in the laboratory at periods of several months by relating the radiometer output voltage to the temperature of a blackbody source as it is cycled from ambient ($\approx$295 K) down to about 205 K. This temperature variation is achieved by incrementally adding dry ice to a bath of alcohol (Shaw and Fedor 1993). There is no common hardware or software in the PRT5 and FTIR calibrations.

In the field, the PRT5 is mounted in a metal box mounted on the ceiling of our mobile radiometer trailer, viewing the atmosphere continuously. Rain and other contaminants are kept out by a fan that blows air around the radiometer and outward through the roof hole. The PRT5 voltage is integrated for 30 or 5 s, depending on the atmospheric conditions, and converted to an equivalent brightness temperature through a third-order polynomial fit derived from the laboratory calibration.

The PRT5's electronics were designed originally to provide a linear voltage–temperature response in three narrow temperature ranges selected with a front-panel switch. We have modified the electronics to provide high gain at the low-temperature end without saturating the ambient temperature response. The result is an amplifier response function that relates output voltage to temperature nonlinearly. The uncalibrated cold-temperature tail of the third-order calibration curve deviates rapidly from the true response, causing the cold PRT5 readings to be too warm.

## 3. Data comparison

### a. *Processing of raw measurements*

To match the two instruments spectrally, we multiply the FTIR spectral radiances by the width of a spectral resolution bin to obtain radiances, convert the wavenumber scale ($cm^{-1}$) to a wavelength scale ($\mu$m), and integrate the FTIR radiances with the PRT5 filter transmission function, as indicated in Eq. (1):

$$L_{\text{int}} = \frac{\sum_i (L_i^{\bar{\nu}} \Delta\bar{\nu}) T_{\text{PRT5}}(\lambda_i)}{\sum_i T_{\text{PRT5}}(\lambda_i)}. \quad (1)$$

In Eq. (1), $L_{\text{int}}$ is the integrated FTIR radiance, $L_i^{\bar{\nu}}$ the measured spectral radiance per wavenumber $\bar{\nu}$ ($cm^{-1}$) corresponding to wavelength $\lambda_i$, $\Delta\bar{\nu}$ the FTIR wavenumber spectral resolution, and $T_{\text{PRT5}}(\lambda_i)$ the transmittance of the PRT5 filter at wavelength $\lambda_i$. The result is an integrated FTIR radiance that is spectrally weighted in the same way as the PRT5 measurement. We convert this to an equivalent brightness temperature by iterative integrations of the Planck function over the PRT5 spectral band. Finally, to make the two measurements temporally equivalent, we average the PRT5 readings over the FTIR integration time.

Figure 1 is a scatterplot of the brightness temperatures from the FTIR ($Tb_{\text{FTIR}}$) and from the PRT5 ($Tb_{\text{PRT5}}$). The agreement of the measurements for temperatures down to about 205 K is pleasing, considering the fundamentally different instruments involved and the fact that all the data were collected in a mostly unattended field-operation mode during all types of weather conditions. However, below 205 K the PRT5 reads increasingly warmer than the FTIR.

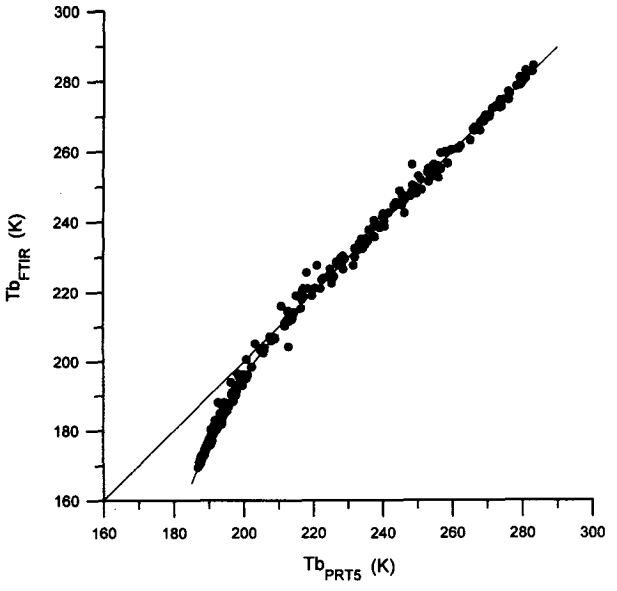


FIG. 1. Scatterplot of the brightness temperatures measured by the FTIR and PRT5. The data include all 403 FTIR measurements collected during the FIRE II experiment. Agreement degrades below 205 K, the cold cutoff of the PRT5 calibration. Included are best-fit curves for the regions above and below 205 K.

The current PRT5 calibration procedure covers from ambient temperature (≈295 K) down to only about 205 K. The PRT5 calibration curve is a third-order polynomial fit to the radiometer voltages plotted versus calibration-source temperature. Below the low-temperature calibration cutoff of 205 K, the calibration curve departs from the true voltage–temperature relationship, making the cold-temperature PRT5 readings increasingly too warm.

### *b. Comparison of data after PRT5 cold-calibration correction*

To extend the cold PRT5 calibration, we divided the raw dataset into two parts: one for $Tb_{FTIR} \geq 205$ K and the other for $Tb_{FTIR} < 205$ K. The best-fit curves for these two parts of the scatterplot are shown in Fig. 1. As shown in Eq. (2), a quadratic curve fits the cold region, and a straight-line fits the warm region:

$$Tb_{FTIR} = \begin{cases} -0.032273Tb_{PRT5}^2 + 14.4607Tb_{PRT5} \\ \qquad - 1405.7, \quad <205\text{ K} \\ 1.0010Tb_{PRT5}, \quad \geq 205\text{ K}. \end{cases} \quad (2)$$

Subtracting from the original $Tb_{PRT5}$ the difference of these two best-fit equations, for each data point having $Tb_{FTIR} < 205$ K, produces the desired cold-corrected data.

Figure 2 is a scatterplot of the data after the PRT5 cold correction; the points above 205 K have not been changed. The entire dataset now has an rms difference of 1.5 K. Here 95% of the data have differences less than 2 K, equal to the sum of the rms calibration uncertainties for the two instruments. The other 5% of the data have differences between 2 and 8 K.

The most likely causes of the differences larger than 2 K are the instruments seeing different portions of the atmosphere and the instruments' responses varying differently over the field of view. Both instruments had 35-mrad fields of view, but they were leveled with respect to each other to within probably 50 mrad, and separated horizontally by about 10 m. The FTIR response appears to fall off faster outside the nominal field of view than the PRT5 response. Thus, inhomogeneous scenes could produce different measurements, even if the radiometers viewed simultaneous regions of the scene.

To understand the significance of the larger temperature differences, we calculated the standard deviation of the PRT5 temporal average for each data point. Twenty-five percent of the points differed by more than three standard deviations of the PRT5 mean and 70% differed by less than two standard deviations. However, all of the differences greater than two standard deviations are smaller than 2 K, and the corresponding standard deviations are near zero (e.g., clear-sky measurements). When we set these near-zero standard deviations equal to the 1 K calibration uncertainty, 90% of the data points were within one standard deviation and the remaining 10% of the points were between one and three standard deviations (only two points differed by between two and three standard deviations). Furthermore, none of the differences larger than 2 K exceeded one temporal standard deviation.

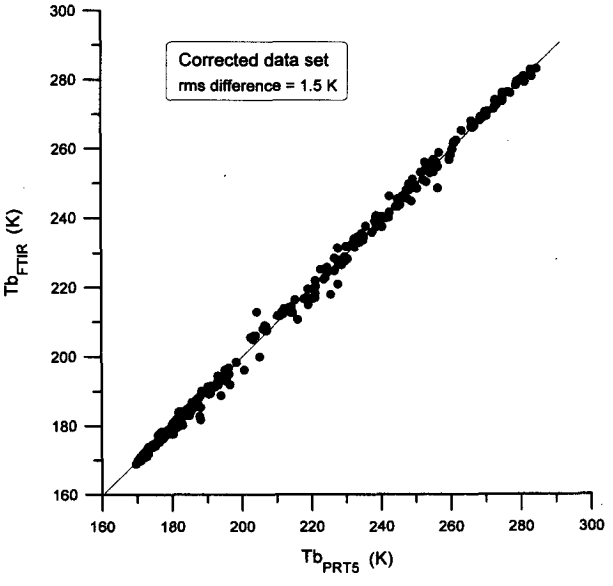


FIG. 2. Scatterplot of the entire dataset after correction of the cold PRT5 measurements by subtracting from $Tb_{PRT5}$ the difference between the warm and cold best-fit lines in Fig. 1.

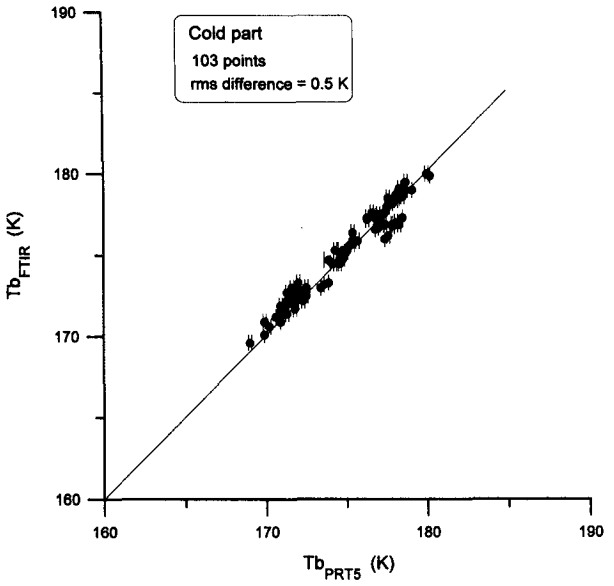


FIG. 3. The cold part of the dataset, corresponding to clear-sky conditions. The error bars indicate the standard deviation of the PRT5 temporal average, as a measure of the temporal stability of each data point. The 0.5-K rms difference is well within the 1-K rms calibration uncertainty for each sensor.

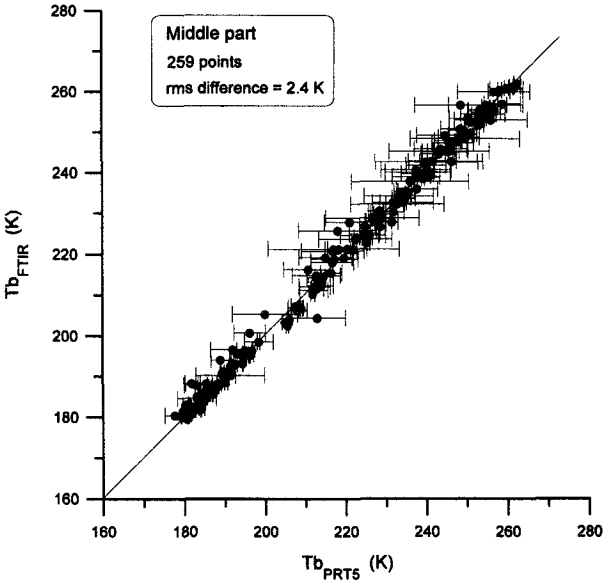


FIG. 4. The middle part of the dataset, corresponding to variable clouds. (Error bars indicate the PRT5 temporal standard deviation.) The 2.4-K rms difference is just greater than the sum (2 K) of the two sensors' rms calibration uncertainties.

To further verify that the FTIR-based correction to the PRT5 data is meaningful, we compared several clear-sky PRT5 readings, before and after correction, with FASCODE3 calculations based on collocated radiosondes. The corrected readings always differed by less than 5 K from the calculations; the uncorrected readings were warm by 15–25 K every time.

### c. *Physical interpretation of three data regions*

There are three distinct regions evident in Fig. 2. In the first region ($Tb_{FTIR} < 180$ K) the data points are tightly distributed with an rms difference of 0.5 K. This region corresponds to clear skies and thin cirrus. Figure 3 is a scatterplot of the data in this cold region, including error bars that indicate the PRT5 temporal standard deviation. The average temporal standard deviation in this region is 0.06 K, and none of these points have a standard deviation larger than 1 K, indicating a high degree of temporal stability.

The second region (180 K $< Tb_{FTIR} <$ 265 K), shown in Fig. 4, corresponds to variable clouds (both convective and cirrus). The numerous temporal standard deviations of 5 K or more indicate the extreme temporal variability of these measurements. It is remarkable that the two instruments measured brightness temperatures in these rapidly varying conditions to within an rms difference of 2.4 K.

The third region (265 K $< Tb_{FTIR}$), shown in Fig. 5, corresponds to relatively uniform clouds, usually stratus. The data in this region contain a large percentage of points with temporal standard deviations on the order of 1–3 K. This is larger than the coldest region but smaller than the middle region. Correspondingly, the rms difference in this region is only 0.8 K, almost as good as that of the coldest region. (Note the scale difference between Figs. 3, 5 and Fig. 4.)

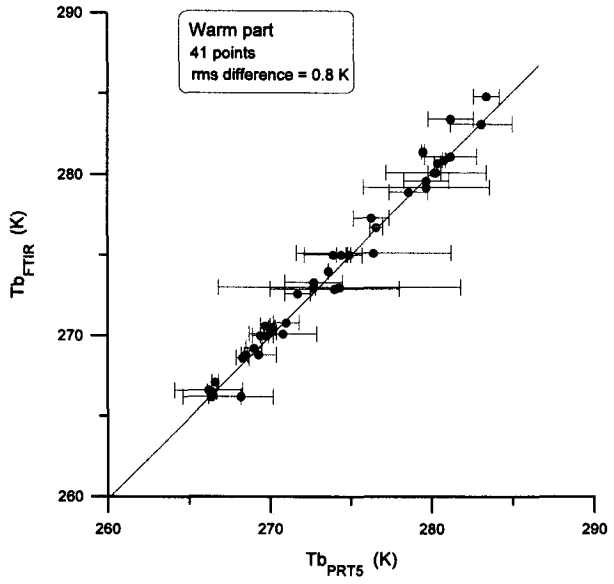


FIG. 5. The warm part of the dataset, corresponding to relatively uniform clouds. The 0.8-K rms difference is within the 1-K calibration uncertainty of each sensor.

## 4. Discussion

Beyond the data subset shown in this paper, we also have corrected the PRT5 measurements from the entire FIRE II dataset (9 November–8 December 1991). Examination of PRT5 calibration curves for the year following FIRE II shows that it is possible to use this correction for those data as well. During a calibration in October 1992 we adjusted the PRT5 amplifier gains, so the correction discussed here is not as good for data collected after that time. Even still, applying this correction to those later data produces errors on the order of 3–10 K, which is much better than the 10–25-K errors that occur with no correction.

This radiometer data validation and correction procedure is of broad interest because of the wide spectral range covered by FTIR spectrometers. The same technique is useful for radiometers having a variety of wavelengths, bandwidths, and filters. We are making such comparisons with other radiometers and have found this technique to be useful for identifying calibration problems.

## 5. Conclusions

We have successfully compared brightness temperatures measured by two fundamentally different infrared radiometers. The well-calibrated FTIR measurements provide a calibration for the originally uncalibrated cold PRT5 measurements. With this correction, the entire dataset exhibits an rms difference of 1.5 K; before the cold correction, the dataset exhibited comparable rms differences down to the PRT5 calibration cutoff of 205 K.

The clear-sky and uniform cloudy data have rms differences less than the calibration uncertainty of 1 K, while the variably cloudy data have an rms difference of 2.4 K due to the large temporal variations of the atmospheric conditions during the measurement periods. All of the data that have temperature differences greater than 1 K are within two standard deviations of the PRT5 temporal average; 90% are within one standard deviation.

The success of this comparison without complicated data processing, outlier removal, or bias removal is encouraging. It suggests that, with the proper care in calibration and operation, fundamentally different instruments are capable of providing quantitatively meaningful radiation measurements that are useful in a variety of atmospheric radiation and cloud physics problems. In addition, the corrected PRT5 measurements show that with proper calibration this relatively simple and inexpensive instrument is capable of providing accurate clear-sky and cirrus emission measurements.

## REFERENCES


Ackerman, S. A., W. L. Smith, J. D. Spinhirne, and H. E. Revercomb, 1990: The 27–28 October 1986 FIRE IFO cirrus case study: Spectral properties of cirrus clouds in the 8–12 $\mu$m window. *Mon. Wea. Rev.*, **118,** 2377–2388.

Grund, C. J., S. A. Ackerman, E. W. Eloranta, R. O. Knutsen, H. E. Revercomb, W. L. Smith, and D. P. Wylie, 1990: Cirrus cloud characteristics derived from volume imaging lidar, high resolution lidar, HIS radiometer, and satellite. *Seventh Conf. on Atmospheric Radiation,* San Francisco, CA, Amer. Meteor. Soc., 357–362.

Matrosov, S. Y., B. W. Orr, R. A. Kropfli, and J. B. Snider, 1994: Retrieval of vertical profiles of cirrus cloud microphysical parameters from Doppler radar and infrared radiometer measurements. *J. Appl. Meteor.*, **33,** 617–626.

Platt, C. M. R., 1973: Lidar and radiometric observations of cirrus clouds. *J. Atmos. Sci.*, **30,** 1191–1204.

——, and A. C. Dilley, 1981: Remote sounding of high clouds. Part IV: Observed temperature variations in cirrus optical properties. *J. Atmos. Sci.*, **38,** 1069–1082.

Revercomb, H. E., H. Buijs, H. B. Howell, D. D. LaPorte, W. L. Smith, and L. A. Sromovsky, 1988: Radiometric calibration of IR Fourier transform spectrometers: Solution to a problem with the High-Resolution Interferometer Sounder. *Appl. Opt.*, **27,** 3210–3218.

Shaw, J. A., and L. S. Fedor, 1993: Improved calibration of infrared radiometers for cloud temperature remote sensing. *Opt. Eng.*, **32,** 1002–1010.

Snider, J. B., 1987: Radiometric observations of cloud liquid water during FIRE. *Proc. IGARSS '88, IEEE,* 261–262.

Spinhirne, J. D., and W. D. Hart, 1990: The 27–28 October 1986 FIRE cirrus case study: ER-2 lidar and spectral radiometer cirrus observations. *Mon. Wea. Rev.*, **118,** 2329–2343.

Uttal, T., S. Y. Matrosov, J. B. Snider, and R. A. Kropfli, 1994: Relationship between ice water path and downward longwave radiation for clouds optically thin in the infrared: Observations and model calculations. *J. Appl. Meteor.*, **33,** 348–357.